

Engineering Applications of Computational Methods 1

S. Arungalai Vendan · Rajeev Kamal ·  
Abhinav Karan · Liang Gao ·  
Xiaodong Niu · Akhil Garg

# Welding and Cutting Case Studies with Supervised Machine Learning

 Springer

# **Engineering Applications of Computational Methods**

Volume 1

## **Series Editors**

Liang Gao, State Key Laboratory of Digital Manufacturing Equipment and Technology, Huazhong University of Science and Technology, Wuhan, Hubei, China

Akhil Garg, School of Mechanical Science and Engineering, Huazhong University of Science and Technology, Wuhan, Hubei, China

The book series Engineering Applications of Computational Methods addresses the numerous applications of mathematical theory and latest computational or numerical methods in various fields of engineering. It emphasizes the practical application of these methods, with possible aspects in programming. New and developing computational methods using big data, machine learning and AI are discussed in this book series, and could be applied to engineering fields, such as manufacturing, industrial engineering, control engineering, civil engineering, energy engineering and material engineering.

The book series Engineering Applications of Computational Methods aims to introduce important computational methods adopted in different engineering projects to researchers and engineers. The individual book volumes in the series are thematic. The goal of each volume is to give readers a comprehensive overview of how the computational methods in a certain engineering area can be used. As a collection, the series provides valuable resources to a wide audience in academia, the engineering research community, industry and anyone else who are looking to expand their knowledge of computational methods.

More information about this series at <http://www.springer.com/series/16380>

S. Arungalai Vendan · Rajeev Kamal ·  
Abhinav Karan · Liang Gao ·  
Xiaodong Niu · Akhil Garg

# Welding and Cutting Case Studies with Supervised Machine Learning

S. Arungalai Vendan  
Department of Electronics and  
Communication, School of Engineering  
Dayananada Sagar University  
Bangalore, India

Abhinav Karan  
School of Engineering  
Dayananada Sagar University  
Bangalore, India

Xiaodong Niu  
Shantou Ruixiang Mould Co. Ltd.,  
Jinping S&T Park  
Shantou, China

Department of Mechatronics Engineering  
Shantou University  
Shantou, China

Rajeev Kamal  
School of Engineering  
Dayananada Sagar University  
Bangalore, India

Liang Gao  
State Key Lab of Digital Manufacturing  
Equipment and Technology  
Huazhong University of Science  
and Technology  
Wuhan, Hubei, China

Akhil Garg  
School of Mechanical Science  
and Engineering  
Huazhong University of Science  
and Technology  
Wuhan, Hubei, China

ISSN 2662-3366

ISSN 2662-3374 (electronic)

Engineering Applications of Computational Methods

ISBN 978-981-13-9381-5

ISBN 978-981-13-9382-2 (eBook)

<https://doi.org/10.1007/978-981-13-9382-2>

© Springer Nature Singapore Pte Ltd. 2020

This work is subject to copyright. All rights are reserved by the Publisher, whether the whole or part of the material is concerned, specifically the rights of translation, reprinting, reuse of illustrations, recitation, broadcasting, reproduction on microfilms or in any other physical way, and transmission or information storage and retrieval, electronic adaptation, computer software, or by similar or dissimilar methodology now known or hereafter developed.

The use of general descriptive names, registered names, trademarks, service marks, etc. in this publication does not imply, even in the absence of a specific statement, that such names are exempt from the relevant protective laws and regulations and therefore free for general use.

The publisher, the authors and the editors are safe to assume that the advice and information in this book are believed to be true and accurate at the date of publication. Neither the publisher nor the authors or the editors give a warranty, expressed or implied, with respect to the material contained herein or for any errors or omissions that may have been made. The publisher remains neutral with regard to jurisdictional claims in published maps and institutional affiliations.

This Springer imprint is published by the registered company Springer Nature Singapore Pte Ltd. The registered company address is: 152 Beach Road, #21-01/04 Gateway East, Singapore 189721, Singapore

# Preface

This book presents machine learning concepts applied in engineering mathematics for applications in advanced welding and cutting processes. Few welding and cutting case studies are presented with details on experimentation and characterization. Subsequently, parametrical interdependencies of various entities governing the processes are investigated using data analysis and data visualization techniques are an embodiment of machine learning. The contents present fundamental and advanced terminologies of supervised learning where focus is laid on Python libraries such as NumPy, Pandas and scikit-learn programming. It emphasizes on the features and benefits of employing machine learning techniques for quantitative analysis of manufacturing processes in the engineering domain. The book exposes the beginners to basics of machine learning for applied sciences, enabling them to acquire requisite knowledge on data sets and its branches for information excavations and adapt to the global competitiveness and work on real-time technical challenges of data. Besides, it also acts as a valuable resource for scholars with ample domain knowledge using conventional mathematical tools for data analysis.

Bangalore, India  
Bangalore, India  
Bangalore, India  
Wuhan, China  
Shantou, China  
Wuhan, China

S. Arungalai Vendan  
Rajeev Kamal  
Abhinav Karan  
Liang Gao  
Xiaodong Niu  
Akhil Garg

# Contents

<b>1 Supervised Machine Learning in Magnetically Impelled ARC BUTT Welding (MIAB)</b> . . . . .	1
1.1 Introduction . . . . .	1
1.2 Process Principle . . . . .	1
1.3 Process-State of Art . . . . .	6
1.3.1 Preliminary Explorations on MIAB Welding Process . . . . .	6
1.3.2 Design/Developmental Aspects in MIAB Welding Process . . . . .	13
1.3.3 Studies on Modelling and Simulation of MIAB Welding Process . . . . .	15
1.3.4 Applications of MIAB Welding . . . . .	16
1.4 Experimentation and Process Governing Parameters . . . . .	18
1.4.1 Miab Equipment . . . . .	18
1.4.2 Specimen for Experimental Trials on MD1 MIAB Machine . . . . .	20
1.4.3 Trials Conducted Using MD1 Machine . . . . .	21
1.4.4 ARC Monitoring During MIAB Welding . . . . .	25
1.4.5 Inferences . . . . .	28
1.4.6 Results and Discussions . . . . .	29
1.5 Parametric Analysis Using Machine Learning Terminologies . . . . .	37
1.5.1 Data Analysis Using <i>NumPy</i> and <i>Pandas</i> . . . . .	38
1.5.2 Data Visualization Using <i>Seaborn</i> and <i>Matplotlib</i> . . . . .	39
1.5.3 Data Preprocessing Using Scikit-Learn . . . . .	39
1.5.4 Prediction Analysis Using Scikit-Learn . . . . .	43
References . . . . .	55

<b>2</b>	<b>Supervised Machine Learning in Cold Metal Transfer (CMT)</b> . . . . .	57
2.1	Introduction . . . . .	57
2.2	Principle of System Operation . . . . .	57
	2.2.1 Welding Power Sources . . . . .	59
	2.2.2 Different Modes of Operation in CMT . . . . .	60
2.3	Process-State of Art . . . . .	60
2.4	Experimentation and Process Governing Parameters . . . . .	62
	2.4.1 Materials . . . . .	62
2.5	Experimentation . . . . .	63
	2.5.1 CMT Welding Set-up . . . . .	63
	2.5.2 Welding Process Parameters . . . . .	63
	2.5.3 Estimation of Heat Input Calculations . . . . .	65
	2.5.4 Results and Discussions . . . . .	66
2.6	Parametric Analysis Using Machine Learning Terminologies . . . . .	75
	2.6.1 Data Analysis Using <i>NumPy</i> and <i>Pandas</i> . . . . .	75
	2.6.2 Data Visualization Using <i>Seaborn</i> and <i>Matplotlib</i> . . . . .	75
	2.6.3 Data Preprocessing Using Scikit-Learn . . . . .	86
	2.6.4 Prediction Analysis Using Scikit-Learn . . . . .	89
	References . . . . .	117
<b>3</b>	<b>Supervised Machine Learning in Friction Stir Welding (FSW)</b> . . . . .	119
3.1	Introduction . . . . .	119
3.2	Process Principle . . . . .	119
3.3	Process-State of Art . . . . .	120
	3.3.1 Investigations on FSW Process and the Underlying Physics . . . . .	120
	3.3.2 Literature Reports Discussing MATERIAL PARAMETERS Influencing FSW Joints . . . . .	124
	3.3.3 Literature Reports on FSW Process Parametric Effects on the Weld Joints . . . . .	125
3.4	Experimentation . . . . .	127
	3.4.1 Material . . . . .	127
	3.4.2 Reinforcement Particles . . . . .	128
	3.4.3 Preparation, Melting and Casting . . . . .	128
	3.4.4 FSW Machine Setup . . . . .	129
	3.4.5 Process Parameters . . . . .	129
	3.4.6 FSW Tool Geometry . . . . .	129
	3.4.7 Estimation of Heat Generated During Friction Stir . . . . .	130
3.5	Results and Discussion . . . . .	132
	3.5.1 Tensile Strength . . . . .	132
	3.5.2 Metallurgical Properties of Friction Stir Welded AA6061/Sic/B <sub>4</sub> C Composites . . . . .	134



- 3.6 Parametric Analysis Using Machine Learning Terminologies . . . . 138
  - 3.6.1 Data Analysis Using *NumPy* and *Pandas* . . . . . 138
  - 3.6.2 Data Visualization Using *Seaborn* and *Matplotlib* . . . . . 138
  - 3.6.3 Data Preprocessing Using *Scikit-Learn* . . . . . 142
  - 3.6.4 Data Preprocessing Using *Scikit-Learn* . . . . . 149
- References . . . . . 184
- 4 Supervised Machine Learning in Wire Cut Electric Discharge Machining (WEDM) . . . . . 187**
  - 4.1 Introduction . . . . . 187
  - 4.2 Process Principle . . . . . 188
  - 4.3 Process-State of Art . . . . . 189
  - 4.4 Experimentation—Phase I . . . . . 194
  - 4.5 Results and Discussion—Phase I . . . . . 196
    - 4.5.1 Metallographic Analysis . . . . . 196
    - 4.5.2 Wire Properties and Influences on Wire-EDM Performance . . . . . 198
  - 4.6 Experimentation—Phase II . . . . . 199
  - 4.7 Results and Discussion—Phase II . . . . . 199
  - 4.8 Parametric Analysis Using Machine Learning Terminologies . . . . 201
    - 4.8.1 Data Analysis Using *NumPy* and *Pandas* . . . . . 202
    - 4.8.2 Data Visualization Using *Seaborn* and *Matplotlib* . . . . . 202
    - 4.8.3 Data Preprocessing Using *Scikit-Learn* . . . . . 204
    - 4.8.4 Prediction Analysis Using *Scikit-Learn* . . . . . 208
  - References . . . . . 244
- Appendix . . . . . 247**

# Chapter 1

## Supervised Machine Learning in Magnetically Impelled ARC BUTT Welding (MIAB)



### 1.1 Introduction

The MIAB welding process was initially investigated by the E. O. Paton Electric Welding Institute during the 1950s. It was later developed for commercial applications by Kuka Welding systems, who named it the Magnet arc process. Today, MIAB welding is used for a variety of applications throughout Europe and Ukraine [1].

Magnetically impelled arc butt (MIAB) welding is a unique and advanced process which utilizes relatively simple equipment, though based on a set of complex interactions among an arc, an applied magnetic field and also an induced magnetic field. These interactions are accompanied by various changes in terms of arc length, temperature distribution, electromagnetic flux distribution, electrical and mechanical properties of the material, etc. which occur during the heating of the parts being welded. The result is a swift welding process that offers cost savings for a range of joint configurations.

This process is generally employed for thin-walled tubes up to 4 mm in the automobile, machine building, construction and other processing industries. MIAB welding is extensively used in automobile industries in European countries and seldom used in parts of the United States and the United Kingdom.

### 1.2 Process Principle

MIAB welding is a fully automated solid-state welding process. An electric arc is made to strike between two tubes which are aligned in axial direction with a small gap in between. The arc is impelled to move around the joint line by the force of interaction between the arc current and an externally applied magnetic field.

The radial component of the magnetic flux density  $B_r$  and the axial component of the welding arc current  $I_a$  interact with each other exerting a force on the arc [2]. The mathematical expression of this electromagnetic force is given in Eq. (1.1). This force impels the arc along the peripheral edges of the tubes.

$$\vec{F}_{B_r} = K \cdot \vec{I}_a \times \vec{B}_r \quad (1.1)$$

Coefficient  $K$  depends on the value of the arc gap between the two tubes to be welded.

The force exerted on the arc current influences the speed of the rotating arc. Therefore, it is clear that adjusting the strength of the magnetic field, the magnitude of the arc current, or the width of the arc by changing arc current plays an important role on the speed of arc. In particular, by sharply increasing the welding current for a short time just prior to upset, a rapid expulsion of molten metal occurs which enables cleaning action. This eliminates the need for shielding gas.

The rotating arc heats up the peripheral edges of the tubes to cause localized melting and adjacent softening in the heat-affected zone (HAZ) and consequently lowers the yield strength of the adjacent solid material to permit sufficient forging action, a critical aspect of the process. The forging expels most of the molten metal present and a solid phase bond is formed. A basic schematic of MIAB welding is shown in Fig. 1.1, which depicts the welding of two tubes.

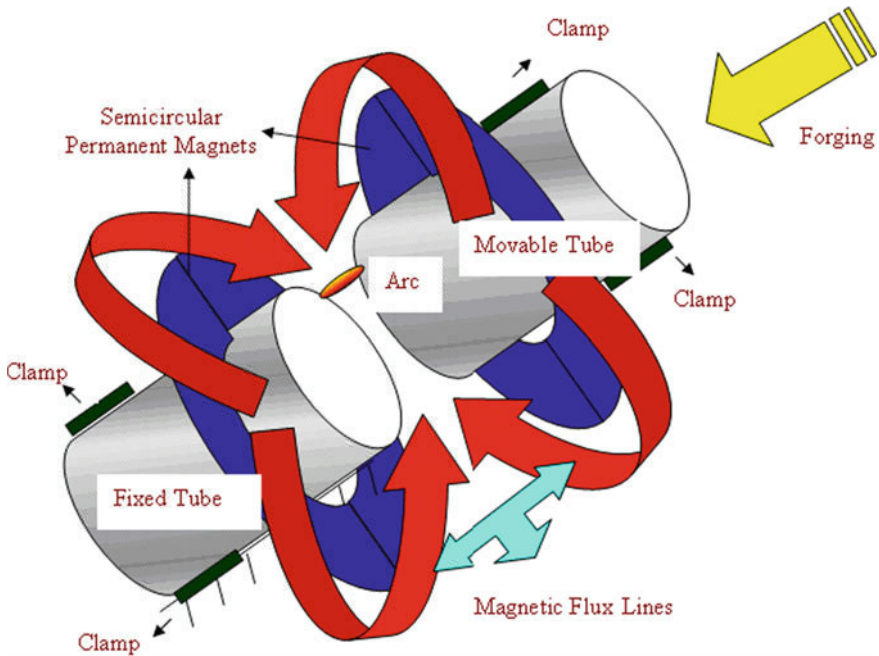


Fig. 1.1 Basic representation of the MIAB welding process

As Fig. 1.1 indicates, an arc is impelled along the peripheral edges of the tubes due to a magnetic field set-up using either permanent magnets or electromagnets. The linear speed of the arc is approximately 250 m/s. The swiftly rotating arc, in combination with the thermal conductivity of the tubes being welded, causes uniform heating at the joint. Subsequently, the molten abutting faces are pressed together by a forging cylinder. This upsetting operation expels the molten material out of the joint and creates a forging action on the remaining plasticized metal. This forging action then forms a porosity-free weld. The process does not use filler material. Shielding gas is usually not required [4]. When shielding gas is not used, as in the case of this research, a short pulse of high current is included which expels contaminated molten metal prior to upset.

MIAB welding is carried out in two stages:

### A. First stage

The first stage of MIAB welding involves co-axial alignment and clamping of the two tubes with a small gap between them. Then a DC current is made to flow through the circuit formed by the power supply, the clamps and the tubes. Further, a carbon rod is employed to strike an arc. Figure 1.3a depicts the situation wherein the arc moves along the tube edges.

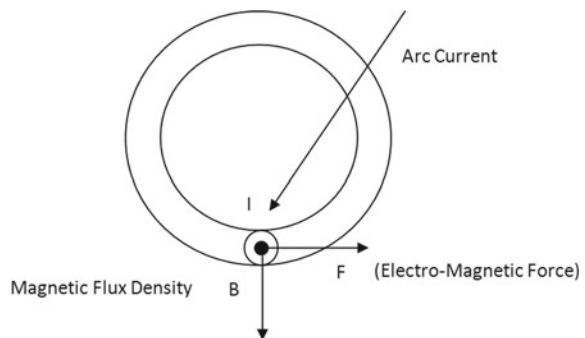
The arc is swivelled along the peripheral edges of the tubes at a high speed. Arc rotation persists for a few seconds until the faying edges are heated to a high temperature, i.e. beyond softening temperature.

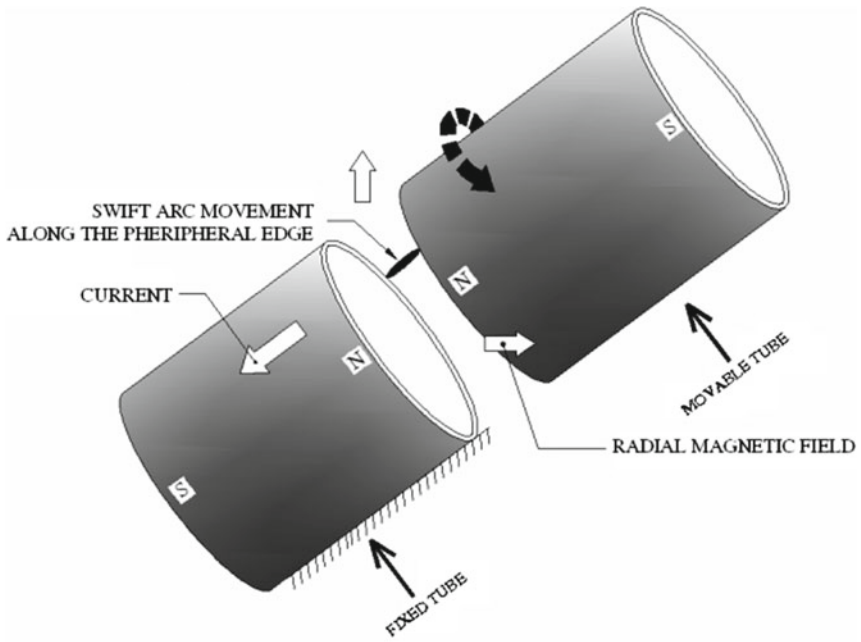
### B. Second stage

After the edges reach a suitable temperature they are pressed together with a pre-determined forging pressure and the weld is set as shown in Fig. 1.3b.

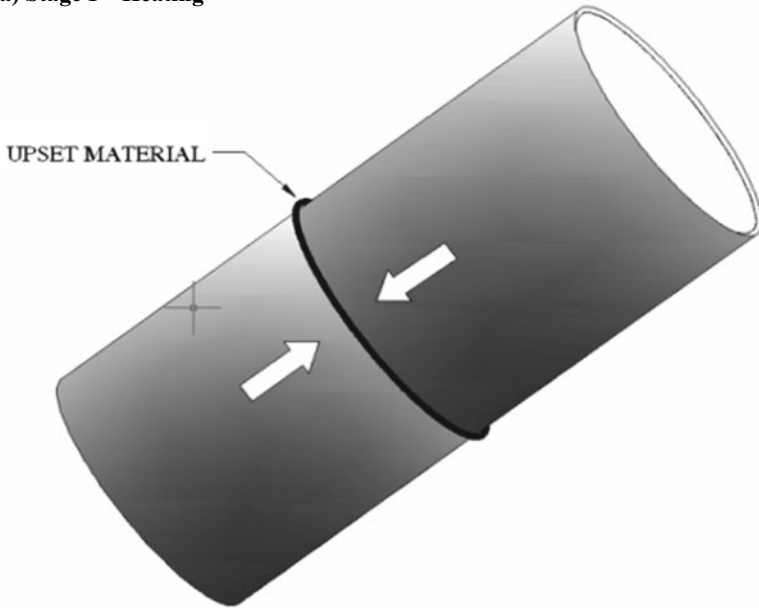
The direction of the force is determined by applying Fleming's left-hand rule, according to which the rotating direction of the arc is always perpendicular to the applied magnetic field and the arc current as shown in Fig. 1.2. The force occurs due to the magnetic flux lines generated by the flowing current interacting with the magnetic flux lines of the applied magnetic field. This phenomenon is shown graphically in Fig. 1.4, which depicts a current carrying conductor under the

**Fig. 1.2** Fleming's left-hand rule [3]





(a) Stage I – Heating



(b) Stage II – Forging

Fig. 1.3 a MIAB welding—heating by arc movement and b MIAB welding—forging

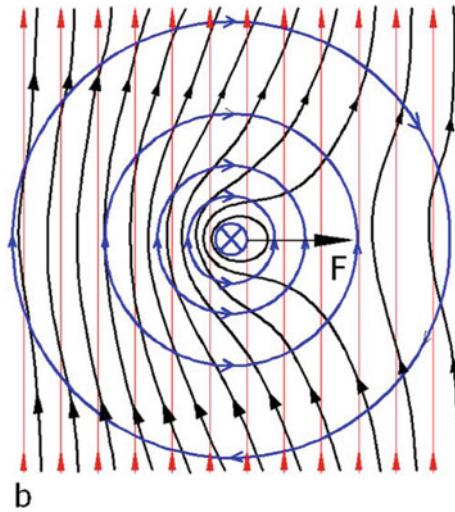


Fig. 1.4 Magnetic field exerting force on current carrying conductor [5]

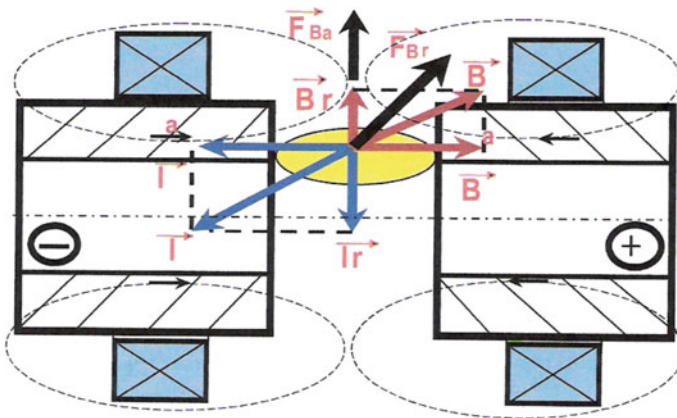


Fig. 1.5 Effect of radial component of arc current on arc movement [2]

influence of an applied magnetic field. The force is generated on the side of the conductor where the magnetic flux lines are dense [5].

In addition to the primary force on the arc that causes the arc to spin rapidly around the part, there is an additional important force on the arc. This force is generated when the radial component of the arc,  $I_r$ , crosses the axial component of the magnetic field  $B_a$ , as shown in Fig. 1.5.

Initially, while MIAB welding a ferromagnetic material, the arc is pushed to the ID of the joint due to arc blow effects. Upon heating, the Curie temperature is first reached on the OD of the tube altering the distribution of magnetic flux in the joint

and pushing the arc outward. The outward movement of the arc can play an important role in generating uniform heating at the joint [2].

### Applications

The range of tube diameters which can be welded on commercially available equipment is approximately 10–220 mm with wall thickness of 0.7–13 mm (7 mm and above has been MIAB welded but with a more complex weld cycle which included the orbital motion of one tube). This comprises different types of tubes and pipes

## 1.3 Process-State of Art

For a researcher investigating MIAB welding with a view to applying, it for welding boiler tubes, the literature available is to some extent, scarce and inadequate. Many of the papers are translated from other foreign languages. In some cases, the translations are not clear; adding to the difficulty in understanding. This chapter presents a comprehensive overview of the earlier research work carried out in the area of MIAB welding. It also reveals the disagreement among various researchers with respect to the underlying concepts of MIAB welding; in particular, the discrepancies pertain to the interaction between the arc and the applied and induced magnetic fields.

### 1.3.1 Preliminary Explorations on MIAB Welding Process

This section reports the initial postulates on MIAB welding process (Table 1.1).

$$T(y, t) = \frac{qy}{2\lambda\pi} \left\{ \left[ \frac{\sqrt{4at}}{y} \exp\left(-\frac{y^2}{4at}\right) - \sqrt{\pi} \left[ 1 - \Phi\left(\frac{y}{\sqrt{4at}}\right) \right] \right] \right\} \quad (1.2)$$

where

T	temperature (°C)
t	arc rotation time (s)
q	heat input of the arc (cal/cm °C)
y	distance from arc along the tube (cm)
$\lambda$	coefficient of thermal conduction (cal/cm s °C)
a	coefficient of temperature conduction (cm <sup>2</sup> /s) and
$\Phi\left(\frac{y}{\sqrt{4at}}\right)$	function of Gauss probability

**Table 1.1** Brief of research reports on MIAB welding process and its technicalities

Authors and year	Experimentation	Observations	Images and equations
Steffen et al. [7]	<ul style="list-style-type: none"> <li>Investigated a variety of conditions and their effect on arc behaviour, including the use of internal and external magnets and different power sources. Steel tubes of various dimensions were used</li> <li>A high speed video camera and an electronic image converter were used to study the arc</li> </ul>	<p>Observations</p> <ul style="list-style-type: none"> <li>Differences in the behaviour of the arc at the anode versus the cathode side of the joint was observed</li> <li>Arc was seen to move freely on the anode side of the joint but was constricted on the cathode side</li> <li>When the arc is forced to move in the presence of a magnetic field, the anode spot is blown ahead while the cathode spot trails</li> <li>Arc always initiate along the inner diameter (ID) of the tube edges. This was due to the fact that the arc tends to move to the regions that heat up quickly and also to areas where the induced magnetic field surrounding the arc encounters the demagnetizing effects due to the applied field</li> <li>It was postulated that as the steel melts on the ID edges, the arc length increases. The longer arc, combined with centrifugal forces pushing the arc outward, results in the arc moving toward the outer diameter (OD) as the welding progresses</li> <li>Internal magnets resulted in faster starting of the weld, but external magnets provided for a more controlled rotation of the arc</li> </ul>	NA
Nentwig et al. [8]	<ul style="list-style-type: none"> <li>Compared the effect of an internal versus external placement of magnetic coils on arc behaviour during MIAB welding of tubes</li> </ul>	<ul style="list-style-type: none"> <li>The maximum radial flux density in the weld gap is always along the edge of the tube closest to the coil</li> <li>When welding ferromagnetic materials, the magnetic flux density drops sharply along the wall thickness of the tube. This affects mainly the arc starting characteristics immediately following arc initiation</li> </ul>	NA

(continued)



Table 1.1 (continued)

Authors and year	Experimentation	Observations	Images and equations
Kachinskiy et al. [2]	<ul style="list-style-type: none"> <li>Investigated the arc behaviour during the welding of hollow parts with wall thickness, greater than 6 mm</li> </ul>	<ul style="list-style-type: none"> <li>It is a challenge to weld thick-walled components due to the tendency of the arc to concentrate on the ID of the component in the MIAB welding process thus resulting in uneven heating</li> <li>The authors postulated that the anode and cathode spot sizes of an arc should be relatively larger than the wall thickness to achieve even heating</li> <li>As shown in Fig. 1.6, arc column traces consume the ID of the thick-walled tubes during the initial stages of welding</li> <li>Upon further heating, the arc column moves to the OD, but the large wall thicknesses prevent stable movement of the arc to the region of higher magnetic field induction leading to non-uniform heating</li> <li>In order to improve this situation, the authors adjusted the position of the magnetic field so as to reinforce the axial component rather than the radial component of the applied magnetic field</li> <li>With this modification, a larger axial magnetic flux component crosses the radial current component of the arc. This, in turn, produces a greater force on the arc, pushing it towards the OD of the tube</li> </ul>	See Fig. 1.6
Kuchuk-Yatsenko et al. [9]	<ul style="list-style-type: none"> <li>Studied the arc behaviour during MIAB welding of a tube to a plate</li> </ul>	<ul style="list-style-type: none"> <li>In this type of joint, the displacement of the arc from the ID to the OD was reportedly more pronounced due to the magnetic blow resulting from the interaction of the arc and the induced magnetic field</li> </ul>	See Fig. 1.7

(continued)

**Table 1.1** (continued)

Authors and year	Experimentation	Observations	Images and equations
Sato et al. [10]	<ul style="list-style-type: none"> <li>• Studied the phenomenon of the arc initiating on the ID of steel pipes and then moving to the OD, especially when welding thick cross-sections</li> <li>• Photo-transistors were used to assess the movement of the arc</li> <li>• Arc traces of the pipe ends were conducted when the arc was initiated on the OD in the presence of an applied magnetic field and in the absence of an applied magnetic field</li> </ul>	<ul style="list-style-type: none"> <li>• This creates a greater concentration of magnetic lines of force on the ID of the tube, which pushes the arc outward as shown in Fig. 1.7. This situation can lead to uneven heating and a poor quality weld</li> <li>• In both cases, the arc moved to the ID of the pipe (Fig. 1.8)</li> <li>• The initial movement of the arc along the ID during the initial arc phase was not due to the arc initiating there, nor was it due to the applied magnetic field pushing it towards the ID. The authors illustrated that a magnetic arc blow effect occurs due to the tube geometry interacting with the magnetic field of the arc. This causes stronger lines of force on the OD of the tube which pushes the arc towards the ID (Fig. 1.9)</li> <li>• The movement of the arc from the ID to the OD at the tube was due to the variations of the magnetic field at the tube ends as the temperature rises with heating</li> <li>• Specifically spontaneous magnetism of iron drops with the temperature and at the Curie temperature (770 °C), iron is no longer considered to be magnetic. This creates a condition in which the magnetic arc blow pushes the arc towards the OD</li> </ul>	See Fig. 1.8 See Fig. 1.9
Yatsenko et al. [11]	<ul style="list-style-type: none"> <li>• Studied the velocity of the arc movement in the gap between a tube and a plate</li> <li>• Specifically, they evaluated the effect of weld parameters and the arc gap variations</li> </ul>	<ul style="list-style-type: none"> <li>• The speed of the arc depends on welding current, the magnetic field intensity, the arc gap and the temperature of the metals being welded</li> <li>• Scale and oxides on the faying surfaces at the joint played a role in arc velocity and mobility. The arc was also</li> </ul>	

(continued)

Table 1.1 (continued)

Authors and year	Experimentation	Observations	Images and equations
	<ul style="list-style-type: none"> <li>• Photoelectric cells and galvanometers were utilized to study the arc movement</li> </ul>	<p>observed to become highly mobile if scale was removed from the plate and tube ends</p> <ul style="list-style-type: none"> <li>• Distinctions between the anode (tube side) and cathode (plate side) spots were discussed</li> <li>• In particular the anode spot was seen to be interrupted, with evidence of jump-like movement, especially in the presence of metal vapours</li> <li>• The speed of the arc increased as the workpiece temperature is increased. It was suggested that this was due to the fact that the area of the anode spot increases with increasing temperature. This reduces the current density and rigidity of the arc plasma, allowing greater distortion of the arc column from the applied magnetic field. The increased distortion promotes the increase of new anode spots, allowing faster movement of the arc</li> <li>• A layer of molten metal soon forms a wave bridge on the tube ends which reduces the gap and consequently, the arc length. The reduced arc length causes stiffer arc plasma, which is more difficult to be moved by the applied magnetic field</li> <li>• This explains the drop in arc velocity after the first peak. The increase in gap then causes another jump in arc velocity. This is due to the decrease in arc stiffness described above</li> </ul>	

(continued)

**Table 1.1** (continued)

Authors and year	Experimentation	Observations	Images and equations
Taneko et al. [12]	<ul style="list-style-type: none"> <li>Studied the relationship between arc velocity, arc angle and the position at which power is supplied to the tubes</li> <li>They used a voltage detector at various locations inside a carbon steel pipe, an oscilloscope and a high speed video camera to measure arc velocities and arc angles</li> </ul>	<ul style="list-style-type: none"> <li>They concluded that due to the arc blow effect and the low electrical resistance of the tube, the current increases in the arc closer to the power supply connection on the tube. This increases the magnetic blow effect and decelerates the arc</li> <li>As the arc moves away from the power supply point, it accelerates. The authors concluded that in order to support a stable moving arc, it is important to have numerous uniform contact points on the tube</li> </ul>	
Xiancong et al. [13]	<ul style="list-style-type: none"> <li>They investigated heat flow in the MIAB weld joint</li> </ul>	<ul style="list-style-type: none"> <li>They considered the rotating arc to be a constant heat source and applied the following heat flow equation for predicting the temperature at time <math>t</math> and distance <math>y</math> from the arc (Eq. 1.2)</li> <li>It was determined that acceptable welds could be achieved at <math>T = 1200\text{ }^{\circ}\text{C}</math> at <math>y = 0.1\text{ cm}</math> or at <math>T = 900\text{ }^{\circ}\text{C}</math> at <math>y = 0.4\text{ cm}</math></li> <li>This formula can also be used to calculate the width of the heat-affected zone</li> </ul>	See Eq. (1.2)
Kalev et al. [14]	<ul style="list-style-type: none"> <li>Investigated heat source (Arc)</li> </ul>	<ul style="list-style-type: none"> <li>That a MIAB welding arc is not a constant, uniform heat source since a typical weld cycle involves different levels of current from the beginning to the end</li> </ul>	NA

**Fig. 1.6** Melting patterns of thick-walled tube reveal melting on ID

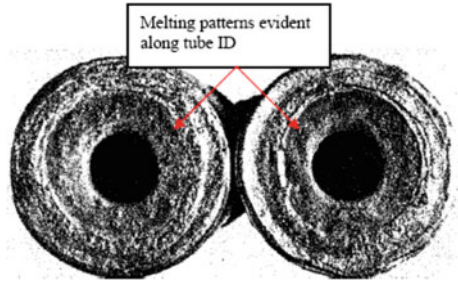


**Fig. 1.7** Magnetic flux in tube-to-plate joint pushes arc outward

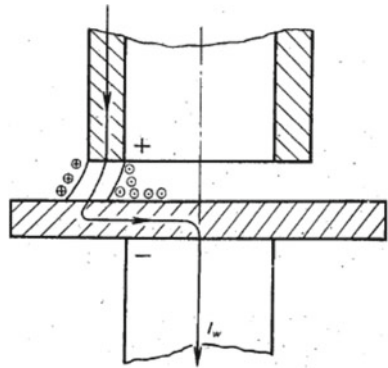


**Fig. 1.8** Arc trace on tube end shows movement from OD to ID

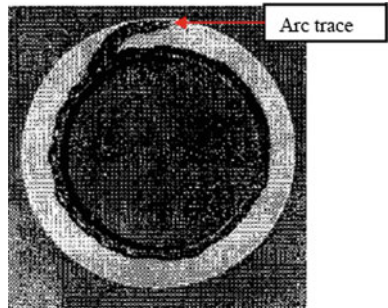


**Fig. 1.9** Magnetic arc blow due to tube geometry effects

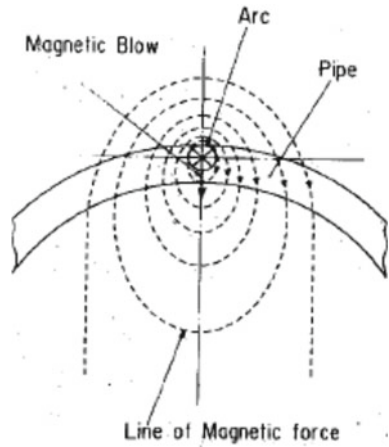


**Fig. 1.10** MIAB set-up with longitudinal small coils

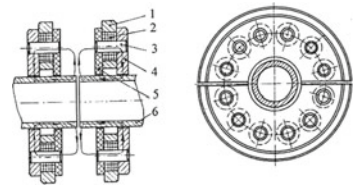
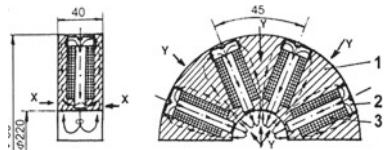


**Fig. 1.11** Transverse magnetizing system



**1.3.2 Design/Developmental Aspects in MIAB Welding Process**

Authors and year	Experimentation	Observations	Images and equations
Georgescu et al. [15]	<ul style="list-style-type: none"> <li>Presented original ROTARC portable equipment, pneumatically operated. The equipment was designed for maximum 30 mm diameter pipes welding. Original pneumatic operating devices</li> </ul>	<ul style="list-style-type: none"> <li>A longitudinal magnetic system design was presented that ensures easy introduction/removal of pipes because the parts were made up of two-halves, due to a system of longitudinal small coils (parallel with the</li> </ul>	See Figs. 1.10 and 1.11

(continued)

(continued)

Authors and year	Experimentation	Observations	Images and equations
	were designed, especially for high speed upset	pipes in Fig. 1.10). They further introduced transverse magnetizing concept system (Fig. 1.11) and its implication	
Edson [16]	<ul style="list-style-type: none"> <li>• Reported the developments aimed at increasing the weldable wall thickness to about 12 mm (150KN-Machine Fig. 1.13)</li> <li>• Limitations that arise while welding tubes with higher wall thickness were highlighted</li> </ul>	<ul style="list-style-type: none"> <li>• The thickness limitation crops up from the arc rotating initially on the inside edge and then predominantly on the outer edge of the tube faces</li> <li>• As a result, uneven heating and consequent poor quality welds are obtained. This radial movement of the arc path occurs with any wall thicknesses but becomes less consistent as wall thickness increases above 5 mm</li> <li>• The second difficulty was to ensure immediate arc rotation in order to avoid local melting and resultant short circuiting</li> </ul>	See Fig. 1.12

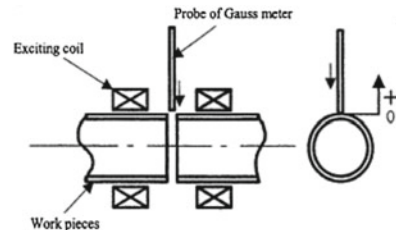
**Fig. 1.12** 150KN MIAB machine and monitoring equipment



### 1.3.3 Studies on Modelling and Simulation of MIAB Welding Process

Authors and year	Experimentation	Observations	Images and equations
Kim and Choi [3]	<ul style="list-style-type: none"> <li>Developed a two-dimensional finite element model for the analysis of magnetic flux density distributions produced by electromagnets at the MIAB weld joint</li> <li>Their experimental set-up, shown in Fig. 1.13, utilized a Gauss-metre at the centre of the joint and the flux density was measured at a varying distance from the outer surface of the pipes at various distances from the exciting coil</li> </ul>	<ul style="list-style-type: none"> <li>It is important to maintain maximum flux density at the joint for best weld quality. Therefore, the design of the electromagnet system is very important, as is the exciting current applied to the electromagnets</li> <li>Both the gap size between the two pipes and the relative permeability of the medium therein had an effect on the magnetic flux at the joint</li> </ul>	See Fig. 1.13
Vendan et al. [17]	<ul style="list-style-type: none"> <li>Performed non-linear electromagnetic analysis to determine the magnetic field and electromagnetic force distribution in MIAB process using finite element package ANSYS</li> <li>Typical results of this analysis pertaining to magnetic field were compared with the experimental data for steel tubes (outer diameter 47 mm and thickness of 2 mm)</li> </ul>	<ul style="list-style-type: none"> <li>The proposed three-dimensional finite element method model for electromagnetic force distribution facilitated comprehensive understanding of the arc rotation process in MIAB welding</li> </ul>	NA

**Fig. 1.13** Method for measuring magnetic flux density





### 1.3.4 Applications of MIAB Welding

Authors and year	Experimentation	Observations	Images and equations
Fletcher et al. [18]	<ul style="list-style-type: none"> <li>A prototype MIAB welding machine was designed and built which was capable of welding natural gas pipelines and to make welds in DN 150 pipe complying with the performance requirements of the Australian petroleum pipeline standard AS2885.2</li> </ul>	<ul style="list-style-type: none"> <li>A typical MIAB welded pipe is shown in Fig. 1.14</li> </ul>	See Fig. 1.14
Tagaki et al. [12]	<ul style="list-style-type: none"> <li>Developed an equipment for rotating arc butt welding suited to pipeline laying in urban areas. The machine was employed to weld pipes of 60.5 mm outside diameter with 3.8 mm wall thickness and 89.1 mm OD with 4.2 mm mild steel town gas pipelines</li> </ul>	<ul style="list-style-type: none"> <li>It was shown that weld quality of high reliability can be obtained with high efficiency and that the welding equipment can be effective in pipeline laying</li> </ul>	NA
Schlebeck [19]	<ul style="list-style-type: none"> <li>Presented the application of MBL-P (Magnetically Moved arc with pressure or MIAB) in engineering components such as CO<sub>2</sub> pressure cylinder for fire extinguishers, pipe screw joint for hydraulic lines and pipe/flange joints of 32–85 mm nominal width.</li> </ul>	<ul style="list-style-type: none"> <li>Figure 1.15 shows the MBL welded CO<sub>2</sub> pressure cylinder for fire extinguishers for which the cycle time is 20 s. The test pressure amounts to 40 MN/mm<sup>2</sup></li> <li>Figure 1.16 shows a full-size MBL welded pipe screw coupling for a hydraulic line with operating pressures up to 15 MN/m<sup>2</sup></li> </ul>	See Fig. 1.15 See Fig. 1.16
Westgate and Edson [20]	<ul style="list-style-type: none"> <li>Outlined the typical industrial applications within the automotive industry</li> </ul>	<ul style="list-style-type: none"> <li>The application of MIAB welding to weld parts in Ford Transit car rear axle casing containing two circular and two square butt welds (Fig. 1.17)</li> </ul>	See Fig. 1.17
Hagan et al. [21]	<ul style="list-style-type: none"> <li>Summarized their use of MIAB welding in the manufacturing of the Fiesta rear axle cross tube assembly</li> <li>In selecting MIAB welding, they first considered the other more common welding methods, viz., Friction, Flash and GMAW</li> </ul>	<ul style="list-style-type: none"> <li>Friction was not acceptable because of the difficulty in maintaining the radial relationship between the shaped flange spindles and the axle tube</li> </ul>	

(continued)

(continued)

Authors and year	Experimentation	Observations	Images and equations
Hiller et al. [22]	<ul style="list-style-type: none"> <li>Used MIAB (in this case, Magnet arc) welding in the production of truck cab suspension components</li> </ul>	<ul style="list-style-type: none"> <li>This application involved MIAB welding a cast iron lever to an extruded steel torsion tube to produce the welded assembly (Fig. 1.18)</li> <li>The authors commented on the many advantages of this process, including short welding times and the excellent mechanical properties of the solid-state joint produced between cast iron and steel</li> </ul>	See Fig. 1.18
Jenicek et al. [23]	<ul style="list-style-type: none"> <li>Demonstrated that tubular hollow bodies such as nuts, sleeves and bushes could be fastened to sheets using a process with particular economic viability, i.e. an advanced variant of magnetically impelled arc butt welding-bush or nut welding</li> </ul>	<ul style="list-style-type: none"> <li>With extended drawn-arc stud welding devices, aluminium components with an internal thread between M8 and M24 were welded on to perforated sheets made of ENAW-<math>AlMg_3</math> and ENAW-<math>AlMgSi_1</math></li> </ul>	NA
Mori et al. [24]	<ul style="list-style-type: none"> <li>Evaluated the feasibility of the MIAB welding process with aluminium and aluminium-copper joints</li> <li>In this set-up, it was a challenge to achieve the required flux density at the joint with non-ferrous materials versus ferrous materials. Hence, an iron core was often inserted inside the pipe</li> </ul>	<ul style="list-style-type: none"> <li>Results achieved showed good weld strength and metallurgical integrity</li> </ul>	NA

**Fig. 1.14** MIAB welded pipes



**Fig. 1.15** MBL welded CO<sub>2</sub> pressure cylinder for fire extinguishers

